Glucagon Increases Retinal Rod Bipolar Cell Inhibition Through a D1 Dopamine Receptor-Dependent Pathway That Is Altered After Lens-Defocus Treatment in Mice

Felipe Tapia,[1,2] Valentín Peñaloza,[1] Francisco Silva-Olivares,[3] Ramón Sotomayor-Zárate,[3] Oliver Schmachtenberg,[1,4] and Alex H. Vielma[1]

[1]Centro Interdisciplinario de Neurociencia de Valparaíso (CINV), Universidad de Valparaíso, Valparaíso, Chile
[2]Programa de Doctorado en Ciencias, Universidad de Valparaíso, Valparaíso, Chile
[3]Laboratorio de Neuroquímica y Neurofarmacología, Centro de Neurobiología y Fisiopatología Integrativa (CENFI), Instituto de Fisiología, Universidad de Valparaíso, Valparaíso, Chile
[4]Instituto de Biología, Facultad de Ciencias, Universidad de Valparaíso, Valparaíso, Chile

Correspondence: Oliver Schmachtenberg, Instituto de Biología, Facultad de Ciencias, Universidad de Valparaíso, Av. Gran Bretaña 1111, Valparaíso 2360102, Chile; oliver.schmachtenberg@uv.cl.
Alex H. Vielma, Centro Interdisciplinario de Neurociencia de Valparaíso (CINV), Universidad de Valparaíso, Pje. Harrington 287, Valparaíso 2381850, Chile; alex.vielma@uv.cl.

Received: October 3, 2023
Accepted: January 5, 2024
Published: January 30, 2024

Citation: Tapia F, Peñaloza V, Silva-Olivares F, Sotomayor-Zárate R, Schmachtenberg O, Vielma AH. Glucagon increases retinal rod bipolar cell inhibition through a D1 dopamine receptor-dependent pathway that is altered after lens-defocus treatment in mice. *Invest Ophthalmol Vis Sci.* 2024;65(1):46. https://doi.org/10.1167/iovs.65.1.46

Purpose. Members of the secretin/glucagon family have diverse roles in retinal physiological and pathological conditions. Out of them, glucagon has been associated with eye growth regulation and image defocus signaling in the eye, both processes central in myopia induction. On the other hand, dopamine is perhaps the most studied molecule in myopia and has been proposed as fundamental in myopia pathogenesis. However, glucagonergic activity in the mammalian retina and its possible link with dopaminergic signaling remain unknown.

Methods. To corroborate whether glucagon and dopamine participate together in the modulation of synaptic activity in the retina, inhibitory post-synaptic currents were measured in rod bipolar cells from retinal slices of wild type and negative lens-exposed mice, using whole cell patch-clamp recordings and selective pharmacology.

Results. Glucagon produced an increase of inhibitory post-synaptic current frequency in rod bipolar cells, which was also dependent on dopaminergic activity, as it was abolished by dopamine type 1 receptor antagonism and under scotopic conditions. The effect was also abolished after 3-week negative lens-exposure but could be recovered using dopamine type 1 receptor agonism.

Conclusions. Altogether, these results support a possible neuromodulatory role of glucagon in the retina of mammals as part of a dopaminergic activity-dependent synaptic pathway that is affected under myopia-inducing conditions.

Keywords: glucagon, myopia, dopamine, retina, bipolar cells

Multiple members of the secretin/glucagon family have been studied in the retina regarding their roles in diverse physiological and pathological processes.[1–4] Out of these molecules, the titular glucagon has been linked with the regulation of eye size[2] and the development of myopia.[5] Myopia is a common refractive error, and its prevalence has steadily increased in recent decades,[6] with higher myopia progression observed after the global confinement measures imposed due to the severe acute respiratory syndrome coronavirus 2 pandemic.[7] Glucagon exhibits protective properties against myopia, decreasing the rate of eye elongation.[8,9] The production of glucagon in the retina has been linked to glucagonergic amacrine cells,[3] with a subgroup of these cells also being immunoreactive for the immediate early gene ZENK, and responding to the sign of image defocus with its downregulation in the chicken myopia model.[10,11] In the case of mammals, mice knocked-out (KO) for Egr-1 (the mammalian ortholog for ZENK) show myopic changes in their refractive characteristics and eyes with greater axial length,[12] and in both rhesus macaques and guinea pigs, a bimodal change in Egr-1 expression is seen, with a decrease under myopia induction and an increase in the opposite condition.[13,14]

On the other hand, dopamine (DA) is perhaps the most researched molecule regarding myopia and is proposed as the main signaling molecule involved in its pathogenesis.[15] In the retina, dopamine is released by dopaminergic amacrine cells, in a process dependent on illumination levels.[16] In general, the use of nonselective dopamine receptor agonists, such as apomorphine, inhibits the development of myopia.[17] More specifically, dopamine D1 receptor (D1R) agonism seems not to affect myopia development,[18,19] whereas its antagonism limits the protective effects of unrestricted vision.[20] Conversely, dopamine D2 receptor

(D2R) agonism has been shown to inhibit myopia development,[18,19] whereas it also prevents the protective effects of unrestricted vision and apomorphine,[18] although D2R antagonism alone does not seem to be sufficient for myopia induction.[21]

In mouse studies, the relationship between myopia and retinal dopamine levels is less explicit compared to other species.[22,23] However, manipulating dopaminergic activity affects eye growth similarly, with agonists generally reducing it[24] and antagonists promoting the opposite effect.[25] Both dopamine receptor families, D1R and D2R, are implicated in murine myopia development. D1R is involved in the protective aspects of apomorphine,[26] inhibiting myopia progression through its agonism,[27] although D1R KO does not alter the trajectory of myopia.[27] Conversely, D2R agonism curtails axial elongation,[28,29] yet selective D2R KO is insufficient to trigger myopia.[28]

Thus, the available data suggest dopamine and glucagon to be two key players in myopia development. However, no studies have reported a direct relationship between dopaminergic and glucagonergic signaling at the retinal level to date, although there are studies in chickens linking dopamine with the expression of ZENK. Intravitreal injection of a nonselective dopaminergic agonist reverted the decrease in ZENK levels observed in myopia, leading to an increase in its expression compared to controls.[11,30]

At the cellular level, functional rod photoreceptors have been reported as necessary for normal refractive eye development.[31] Rods transmit visual information through rod bipolar cells (RBCs), which are regulated by inhibitory activity arising from diverse amacrine cells, depending on the level of light adaptation of the retina.[32] The degree of light adaptation is in turn correlated with the levels of dopaminergic activity, and it has been shown that dopamine acting through D1R decreases the frequency of spontaneous inhibitory activity in RBCs.[33] Furthermore, expression of ZENK/EGR-1 has also been associated to RBCs in chickens and rhesus macaque.[13,34]

The present study thus set out to record the dopamine-regulated inhibitory activity of RBCs, to test whether glucagon plays a role in the modulation of this activity in the mouse retina, both in wild type animals and after negative lens exposure.

Methods

Animals

Experiments were conducted on C75BL/6 mice, regardless of sex and weight at 32 to 48 days of age. The animals were housed in the institutional animal facility of the Universidad de Valparaíso in a controlled environment (20–25°C temperature, 12-hour photoperiod, water and food ad libitum). Procedures were conducted with approval and according to the norms of the bioethics committee of the Universidad de Valparaíso (BEA151-19, BEA169-21, and CBC 06/2020) and following the ARVO Statement for the Use of Animals in Ophthalmic and Vision Research.

Retinal Slices

Animals were deeply anesthetized by isoflurane inhalation and euthanized via decapitation. Eyes were enucleated and kept in extracellular solution composed of (in mM): 119 NaCl, 23 $NaHCO_3$, 1.25 NaH_2PO_4, 2.5 KCl, 2.5 $CaCl_2$, 1.5 $MgSO_4$, 20 glucose, and 2 Na^+ pyruvate, and aerated with 95% O_2 and 5% CO_2 (pH 7.4). The retina was separated from the choroid-sclera, embedded in type VII agarose (Sigma) and retinal slices (200 µm thickness) were obtained using a vibratome (VT1000S, Leica Microsystems).

Patch-Clamp Recordings

Inhibitory activity was recorded from RBCs voltage clamped at 0 mV using recording pipettes pulled from borosilicate capillaries (10–15 MΩ, 1.5 mm OD, 0.84 mm ID, World Precision Instruments) and filled with intracellular solution composed of (in mM): 125 K^+ gluconate, 10 KCl, 10 HEPES, 2 EGTA, 2 Na_2ATP, 2 NaGTP, and 1% Lucifer Yellow (pH 7.4 adjusted with KOH). Signals were processed using an EPC 7 Plus (HEKA Instruments) amplifier, filtered at 3 kHz, digitized and sampled at 10 kHz (Digidata 1440A, Molecular Devices) and recorded using pClamp 10.4 (Molecular Devices). The calculated liquid junction potential of 14 mV was corrected before the recordings. The access resistance was assessed periodically, and recordings were discarded if a variation larger than 15% was observed.

RBCs were visualized under an Eclipse FN1 (Nikon) microscope, equipped with a 40× water immersion objective, using infrared light and differential interference contrast, and a TCH-1.4LICE (Tucsen Photonics) camera. RBCs were identified using the Lucifer Yellow dye dialyzed through the recording pipette, based on their characteristic morphology with a soma in the upper inner nuclear layer (INL) and an axon extending to the limit between the inner plexiform layer (IPL) and the ganglion cell layer, ending in multiple varicosities.[35] During the recordings, it was also possible to assess voltage-gated currents, using a protocol consisting of increasing 10 mV steps between −100 and 50 mV, which has been previously used to identify bipolar cell subtypes.[36] RBCs showed a characteristic pattern under this protocol, with a positive deflection at the start of the −20 mV pulse corresponding to the reciprocal feedback from A17 amacrine cells.[37]

Unless stated otherwise, recordings were performed in photopic conditions. For scotopic experiments, mice were dark-adapted for a period of 2 hours prior to the experiments, which were then conducted under red light of approximately 10 lux measured with a digital luxmeter (LX1330B, Dr. Meter).

Pharmacology

To elicit inhibitory postsynaptic currents (IPSCs), as this activity is significantly decreased in photopic conditions,[32] stimulation was performed using microperfusion of high-potassium extracellular solution (HK-ECS), as previously described,[38] applied to the outer plexiform layer (OPL) from a single-barrel glass pipette operated by a custom-made picospritzer at 2 to 3 psi. HK-ECS contained (in mM): 128 NaCl, 20.1 KCl, 3 $CaCl_2$, 1.2 $MgCl_2$, and 5 HEPES (pH 7.4 adjusted with NaOH). The perfusion was present for the entire duration of the recordings in all subsequent recordings.

To study the role of specific subtypes of activity, pharmacological agents were added to the bath solution as needed. To study the effects of glucagon receptor activity, glucagon and L168,049 were used as agonist and antagonist, respectively. To assess the role of the dopaminergic system, we used SCH 23390 as a D1R antagonist, sulpiride as a D2R

Investigative Ophthalmology & Visual Science

antagonist and SKF 81297 as a D1R agonist. Glucagon was obtained from Sigma, whereas the remaining pharmacologic agents were obtained from Tocris.

HPLC Retinal DOPAC and DA Content Measurements

Animals were deeply anesthetized by isoflurane inhalation and euthanized via decapitation. Eyes were enucleated and kept in phosphate-buffered saline, and the retina was separated from the choroid-sclera. For light-exposed retinas, the extraction was performed under photopic conditions during the 10 minutes required for the procedure. For dark-adapted retinas, animals were dark-adapted for 2 hours, and the extraction procedure was performed under red light of approximately 10 lux measured with a digital luxmeter (LX1330B, Dr. Meter). After extraction, the retinas were stored in 650 µL tubes, covered in foil in the case of dark-adapted retinas, weighed on an analytical scale, snap-frozen, and then stored at −80°C before measurements.

Retinas were weighed on an analytical scale and homogenized in 200 µL of 0.2 M perchloric acid using a sonicator (XL2005, Microson Ultrasonic Cell Disruptor, Heat Systems). The homogenate was centrifuged at 12,000 g for 10 minutes at 4°C (Z233MK-2, Hermle Labor Technik GmbH) and the supernatant was filtered (EW-32816-26; 0.2 µm, HPLC Syringe Filters PTFE, Cole-Parmer). Then, 10 µL of supernatant were injected to an HPLC-ED system with an isocratic pump (PU-2080 Plus, Jasco Co. Ltd.), a C18 column (Kromasil 100-3.5-C18, AkzoNobel), and an electrochemical detector (LC-4C, BAS) set at 650 mV, 0.5 nA. The mobile phase, containing 0.1 M NaH_2PO_4, 1.0 mM 1-octanesulfonic acid, 1.0 mM EDTA, and 8.0% (v/v) CH_3CN (pH 3.4) was pumped at a flow rate of 0.2 mL/min.

DA and DOPAC levels were assessed by comparing the respective peak area and elution time of the sample with a reference standard and the quantification was performed using a calibration curve for DA and DOPAC (Program ChromPass, Jasco Co. Ltd.).

The pellet of each sample was resuspended in 1 mL of 1M NaOH for protein quantification using the Bio-Rad Protein Assay (Bio-Rad Laboratories, Inc.), with bovine serum albumin as standard, and the readout was performed in a microplate spectrophotometer (Epoch, BioTek Instruments Inc.). The concentration of DA and DOPAC are expressed as pg per mg of protein.

Negative Lens Treatment

Mice were exposed to -10 diopter (D) lenses, positioned in front of one of the eyes at days of age, and kept in place for 3 weeks. The contralateral eye was left without a lens as a control. The lenses were secured using a plastic support glued to the cranium of the animal.

To position the support armature, the mouse was anesthetized via inhalation of isoflurane (4-5%) and kept under a lower dose (1-2%) for the rest of the protocol. An analgesic (carprofen 5 mg/kg s.c.) and an antibiotic (enrofloxacin 10 mg/kg s.c.) were also administered. The surgical area on the head of the animal was shaved and disinfected using 70% ethanol and chlorhexidine. A 1.5 mm diameter incision was opened using a surgical blade to access the cranium. Using dental cement, two screws were affixed to the bone and used as a support for the lens armature. After the surgery, animals were kept for a week with their litter, and then moved to an independent cage. The analgesic and antibiotics were continued for 2 days after surgery. The nails of the animals were kept trimmed to prevent lens scratching.

Data Analysis

Recordings were analyzed using a custom script written in Python 3.8.8, available at https://github.com/FTapiaP/IPSCDetection. The data are first filtered using a third order low pass Butterworth digital filter, and then processed using a peak finding algorithm. The threshold amplitude to detect events is set to 2.0, 2.5, or 3.0 times the average noise sampled from the recording, depending on the signal-to-noise ratio, calculated over the baseline trace obtained using the Noise Median method. The functions used for these steps are contained in the SciPy 1.8.0 and pybaselines 1.0.0 packages.

The event frequency is calculated as the number of events divided by the total recording time and the amplitude as the difference between the peak value of an event and the baseline of the signal at that point. The decay time was used as an approximation of the decay tau and calculated as the time from the peak of the event until the event amplitude has decreased to e^{-1} times the peak amplitude.

Statistical Analysis

Statistical analysis was performed using the software Stata/SE 17.0 and jamovi 2.2.5. The Shapiro-Wilk test and residuals plot after every test were used to assess normal distribution. For parametric tests, comparison of means between the two groups was performed using either paired or unpaired *t*-test and for more than two groups, repeated measures or 1-way ANOVA followed by Tukey test. If either sphericity or homoscedasticity were not met, nonparametric tests were used. For nonparametric tests, comparison of means was performed using either the Wilcoxon signed rank test or Mann–Whitney U test for two groups and the Friedman test for more than two groups, followed by post hoc tests using the Durbin-Conover method.

All graphs were constructed using the Matplotlib version 3.5.0 library. For all tests, the significance level was set a $P = 0.05$. Unless otherwise specified, data are presented as mean ± standard deviation, and sample size values as number of cells recorded.

Results

Application of Glucagon Increases the Frequency of Inhibitory Activity in RBCs

To study the potential role of glucagon as a regulator of retinal activity in mammals, we centered on the inhibitory activity of the RBC microcircuit. To this end, HK-ECS was applied using a pipette directed at the OPL (Fig. 1A), the perfusion was present during the entire recording and reliably produced multiple IPSCs with fast kinetics (Fig. 1B). This stimulation procedure was thus used in all further experiments. Glucagon was then bath-applied at a concentration of 1 µM, which caused an increase in IPSC frequency (control = 1.86 ± 1.35 Hz, and glucagon = 2.42 ± 1.75 Hz,

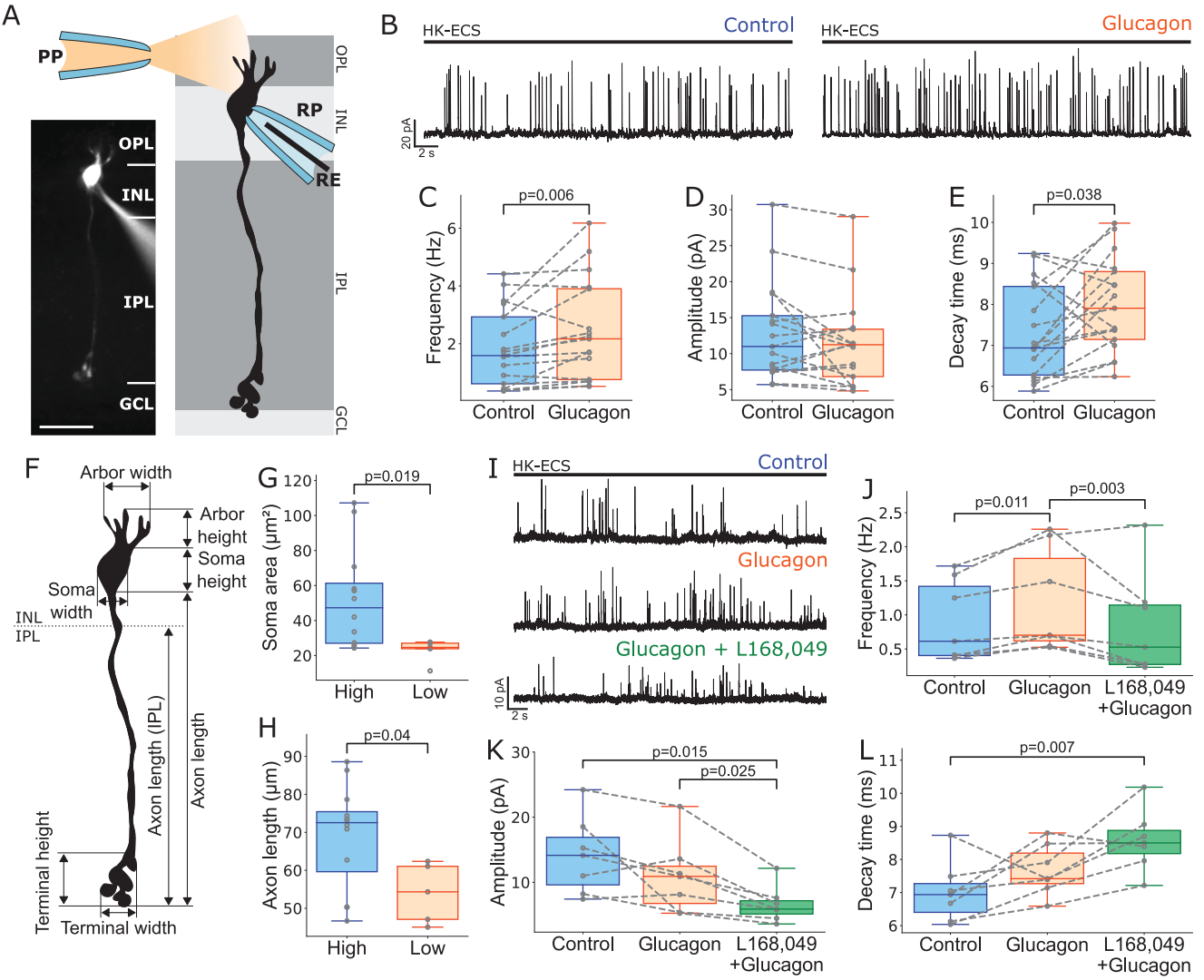

Figure 1. Glucagon application increases the frequency of inhibitory signaling acting on RBCs. (**A**) Schematic representation of the experimental protocol. The whole-cell patch-clamp technique was used to record activity from RBCs and a puffer pipette (PP) was used to administer pharmacological agents to the outer plexiform layer (OPL). RP, recording pipette; RE, recording electrode; INL, inner nuclear layer; IPL, inner plexiform layer; GCL, ganglion cell layer. Scale bar = 20 µm. (**B**) Representative traces of RBC IPSCs under control conditions (*left, blue*) and after 5 minutes of bath application of 1 µM glucagon (*right, orange*). (**C**) Glucagon application produced an increase in the average frequency of IPSCs (paired *t*-test), with no change in IPSC amplitude (**D**), and an increase in average IPSC decay times (Wilcoxon signed-rank test) (**E**). (**F**) Schematic representation of the measurements taken from RBCs. INL, inner nuclear layer; IPL, inner plexiform layer. (**G**) The cells presenting an increase in IPSC frequency of more than 10% compared to baseline after glucagon application (high) were associated with larger soma areas (Mann–Whitney U test) and axon lengths (unpaired *t* test) (**H**), when compared with those presenting less than 10% change (low). (**I**) Representative traces of RBC IPSCs under control conditions (*top, blue*), after 5 minutes of bath application of 1 µM glucagon (*middle, orange*) and after 10 minutes of bath application of 1 µM glucagon + 500 nM L168,049 (*bottom, green*). (**J**) Glucagon application produced an increase in the average frequency of IPSCs, which was abolished with the application of L168,049 (Friedman test with Durbin-Conover pairwise comparisons), co-application of glucagon and L168,049 also produced a decrease in IPSC amplitude (repeated measures ANOVA with Tukey test) (**K**), and an increase in decay time (repeated measures ANOVA with Tukey test) (**L**).

$P = 0.006$, $n = 17$; Figs. 1B, 1C) with no change in average amplitude (Fig. 1D). The events also showed higher decay times (control = 7.32 ± 1.13 ms, and glucagon = 7.98 ± 1.15 ms, $P = 0.038$, $n = 17$; Fig. 1E). When the overall population of cells was studied to assess their behavior when exposed to glucagon, 12 cells showed an increase in frequency above 10% with respect to control (high group = 70.59%) with an average increase rate of 1.67 ± 0.75 times the control condition. As for the cells that showed less than 10% increase or a decrease (low group = 29.41%), the average rate was 0.93 ± 0.15 times the control condition. As these differences in response could suggest the presence of two subpopulations of RBCs based on their glucagon response, it was of interest to correlate the data with the morphological and electrical characteristics of these cells. To this end, measurements of dendrite arborization, soma and axon terminal dimensions, along with axon length, and number of terminal varicosities (Fig. 1F) were correlated with the degree of change observed. A difference was found in soma area (high group = 52.18 ± 28.91 µm², and low group = 22.88 ± 6.7 µm², $P = 0.019$, $n = 17$; Fig. 1G) and axon length (high group = 68.95 ± 13.79 µm, and low group = 53.98 ± 7.87 µm,

$P = 0.04$, $n = 17$; Fig. 1H), although no change was observed in the axon length within the IPL (high group = 49.48 ± 7.03 µm, and low group = 45.08 ± 10.48 µm, $P = 0.32$, $n = 17$).

To test the dependency on glucagon receptor activity of the observed IPSC modulation by glucagon, L-168,049, a selective non-peptidyl glucagon receptor antagonist was used. As was the case with the previous experiments, bath application of 1 µM glucagon induced an increase in the frequency of IPSCs, which was abolished by co-application of 500 nM L-168,048, returning to a frequency not different from control (control = 0.91 ± 0.6Hz, glucagon = 1.2 ± 0.77 Hz, and glucagon + L168,049 = 0.84 ± 0.76 Hz, $P = 0.018$, $n = 7$; Figs. 1I, 1J). Application of 1 µM glucagon did not change the amplitude of the IPSCs, but the subsequent co-application of L-168,049 produced a decrease in IPSC amplitude (control = 14.11 ± 5.95 pA, glucagon = 10.89 ± 5.67 pA, and glucagon + L168,049 = 6.6 ± 2.78 pA, $P = 0.003$, $n = 7$; Fig. 1K). The pooled decay times of IPSCs show a shift towards higher decay times when the control is compared to the co-application of glucagon and L-168,049, with no other differences (control = 7.01 ± 0.92 ms, glucagon = 7.68 ± 0.77 ms, and glucagon + L168,049 = 8.57 ± 0.92 ms, $P = 0.004$, $n = 7$; Fig. 1L). Overall, these results support glucagon as a modulator of the inhibitory signaling acting on RBCs, increasing its frequency through glucagon receptor activation.

The Effect of Glucagon on RBC IPSCs is Dependent on Dopaminergic Signaling

To study a potential interaction between glucagonergic and dopaminergic signaling, the effect of selective antagonism of dopamine receptors on the glucagon-induced increase in IPSC frequency was studied. To this end, 10 µM SCH 23390, a selective dopamine D1R antagonist, was used to isolate the possible effects of D1R signaling, which has been shown to regulate the activity of inhibitory amacrine cells acting upon RBCs.[33,39] The sequential application of SCH 23390 followed by co-application with 1 µM glucagon produced no significant changes in the frequency of IPSCs (control = 3.15 ± 1.85 Hz, SCH = 3.64 ± 1.75 Hz, and SCH + glucagon = 4.58 ± 2.6 Hz, $P = 0.15$, $n = 10$; Figs. 2A, 2B). A decrease in the amplitude of IPSCs was observed with application of SCH 23390 alone, with no difference when it was co-applied with glucagon (control = 8.91 ± 1.84 pA, SCH = 6.48 ± 1.75 pA, and SCH + glucagon = 6.99 ± 2.36 pA, $P = 0.045$, $n = 10$; Fig. 2C). No significant change in the average decay times was observed (Fig. 2D).

Next, to complete the profile of dopaminergic interaction, 10 µM sulpiride, a selective antagonist of D2R was used. Application of sulpiride alone increased IPSC frequency when compared to the baseline, with no change with the addition of glucagon (control = 1.94 ± 1.46 Hz, *sulpiride* = 2.7 ± 1.78 Hz, and sulpiride + glucagon = 3.05 ± 1.8 Hz, $P = 0.013$, $n = 9$; Figs. 2E, 2F). No significant changes were found in the average amplitude of the events (Fig. 2G). In addition, there was a significant increase in the average decay time when sulpiride and glucagon were co-applied (control = 9.78 ± 3.35 ms, sulpiride = 10.6 ± 2.46 ms, and sulpiride + glucagon = 11.56 ± 2.96 ms, $P = 0.038$, $n = 9$; Fig. 2H). Overall, these results support the idea that dopaminergic activity is necessary for glucagon to exert its effect.

The Effect of Glucagon on RBC IPSCs is Absent in Scotopic Conditions

As exogenous dopaminergic antagonism showed an effect over glucagon-mediated modulation, it was of interest to contrast these results with an endogenous hypodopaminergic condition. To this end, recordings of RBC inhibitory activity were performed under scotopic conditions after a period of 2 hours of dark adaptation, which are associated with a decrease in retinal dopamine release.[40] HPLC measurements of retinal dopamine content in this condition confirmed a decrease in total dopamine content (photopic = 3444.42 ± 2878.02 pg/mg of tissue protein, and scotopic = 1007.9 ± 54.97 pg/mg of tissue protein, $P = 0.003$, $n = 12/6$; Fig. 2I). Under these conditions, bath application of glucagon did not produce an increase in the frequency of IPSCs (control = 1.63 ± 1.15 Hz, and glucagon = 2.11 ± 1.2 Hz, $P = 0.193$, $n = 9$; Figs. 2J, 2K). No change was observed in average IPSC amplitudes (Fig. 2L) or decay times (Fig. 2M). This shows a similar profile of the scotopic condition to that of D1R antagonism.

The Increase in IPSC Frequency After Glucagon Application is Abolished in 3-Week Negative Lens-Exposed Mice

Negative lens exposure, an intervention previously used for myopia induction in mice,[41] was used to assess a possible alteration of the glucagon-dopamine interaction observed in RBCs, as both glucagon signaling and dopaminergic disfunction have been linked to myopia development.[24] The intervention consisted in the placement of a –10 D lens over one of the eyes of the animal for a period of 3 weeks, leaving the opposite eye uncovered as a control (Fig. 3A).

The control eye showed characteristics similar to wild type animals, with an increase in IPSC frequency associated with glucagon application (control = 1.09 ± 0.64 Hz, and glucagon = 2.16 ± 1.04 Hz. $P = 0.02$, $n = 5$; Figs. 3B, 3C) and no changes in amplitude (Fig. 3D) or decay time (Fig. 3E). In the case of the treated eye, the increase in frequency was not observed (control = 1.57 ± 0.89 Hz, and glucagon = 1.45 ± 1.33 Hz, $P = 0.84$, $n = 6$; Figs. 3F, 3G). This was associated with a decrease in IPSC amplitude (control = 15.96 ± 4.3 pA, and glucagon = 7.55 ± 2.75 pA, $P = 0.031$, $n = 6$; Fig. 3H), with no change in average decay time (Fig. 3I).

These results suggest that the effect of glucagon is abolished in the eyes of mice exposed to a –10 D lens for a period of 3 weeks.

Dopamine D1R Agonism Recovers Glucagon-Dependent Modulation After 3 Weeks of Negative Lens Exposure

To further characterize the possible link between the dopaminergic disfunction associated with negative lens exposure and the abolition of the effect of glucagon, a selective D1R agonist, SKF 81297, was bath-applied at a concentration of 10 µM.

After 3 weeks of lens exposure, an increase in IPSC frequency was observed in the presence of SKF 81297 alone, with a further increase when glucagon was added (control = 1.63 ± 0.67 Hz, SKF = 2.53 ± 0.75 Hz, and SKF + glucagon = 3.1 ± 1.03 Hz, $P = 0.002$, $n = 7$; Figs. 3J, 3K). This was associated with a decrease in amplitude when SKF and glucagon

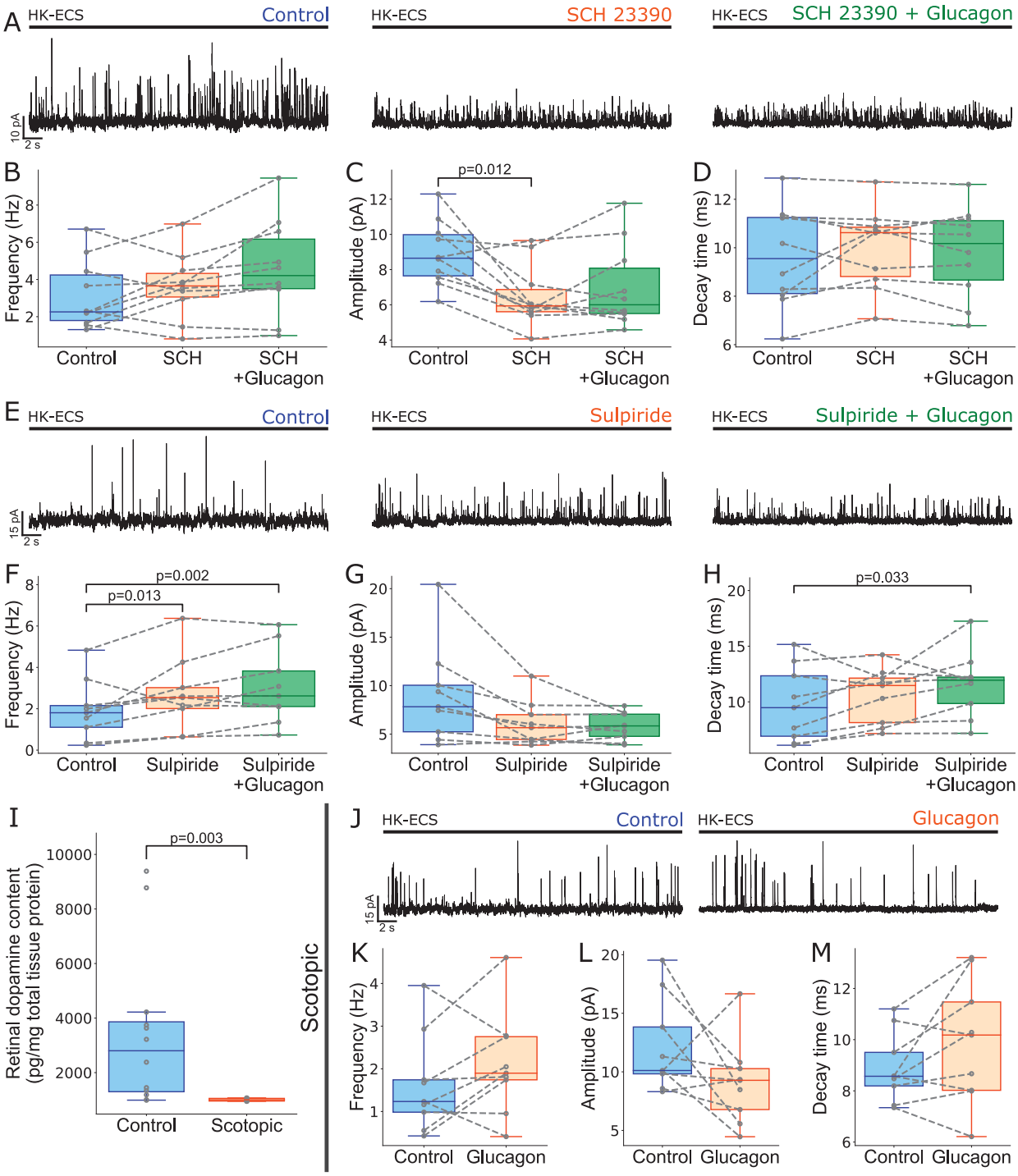

Figure 2. The effect of glucagon application is abolished under dopaminergic antagonism and scotopic conditions. (**A**) Representative traces of RBC IPSCs under control conditions (*left, blue*), after 15 minutes of bath application of 10 µM SCH 23390 (*middle, orange*) and after 5 minutes of bath application of 10 µM SCH 23390 + 1 µM glucagon (*right, green*). (**B**) Application of SCH 23390 alone or co-application with glucagon did not produce changes in average IPSC frequency (Friedman test) and was associated with a decrease in amplitude when SCH 23390 was applied alone (Friedman test with Durbin-Conover pairwise comparisons) (**C**). No changes were observed in decay times (Friedman test) (**D**). (**E**) Representative traces of RBC IPSCs under control conditions (*left, blue*); after 15 minutes of bath application of 10 µM sulpiride (*middle, orange*), and after 5 minutes of bath application of 10 µM sulpiride + 1 µM glucagon (*right, green*). (**F**) Application of sulpiride alone and co-application with glucagon increased average IPSC frequency compared to control (Friedman test with Durbin-Conover pairwise comparisons). No change was observed in average amplitude (Friedman test) (**G**). An increase was observed in decay times when sulpiride and glucagon were co-applied (repeated measures ANOVA with Tukey test) (**H**). (**I**) Retinal dopamine content was measured using HPLC in both photopic (control) and scotopic conditions. A significant decrease was observed in scotopic conditions (unpaired *t* test). (**J**) Representative traces of scotopic recordings of RBC IPSCs under control conditions (*left, blue*) and after 5 minutes of bath application of 1 µM glucagon (*right, orange*). (**K**) No change was observed in the average frequency of IPSCs (paired *t* test), their amplitudes (paired *t* test) (**L**) or decay times (paired *t* test) (**M**).

Investigative Ophthalmology & Visual Science

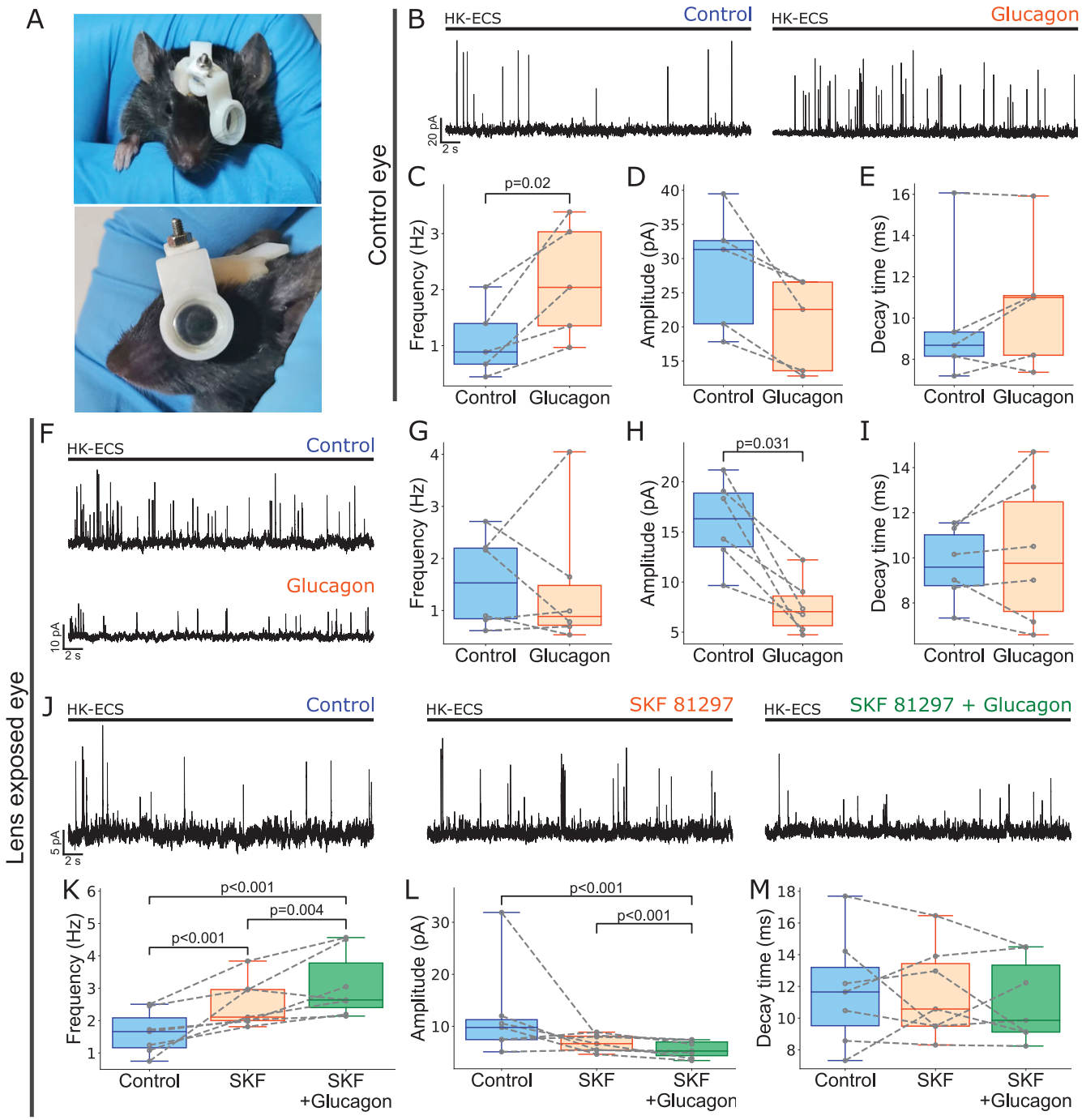

Figure 3. The effect of glucagon is abolished after 3-week negative lens exposure and can be recovered using D1R agonism. (**A**) Image of the lens supporting armature in situ. The frontal view shows the attachment to the skull using a screw glued with dental cement (*top*). The left eye is covered with a -10 D lens, leaving the right eye as a control (*bottom*). (**B**) Representative traces of RBC IPSCs under control conditions (*left, blue*) and after 5 minutes of bath application of 1 µM glucagon (*right, orange*), in the control eye of a 3-week negative lens-exposed mouse. (**C**) An increase was observed in the average IPSC frequency (paired *t* test), with no changes in amplitude (Wilcoxon signed-rank test) (**D**) or decay time (Wilcoxon signed-rank test) (**E**). (**F**) Representative traces of RBC IPSCs under control conditions (*top, blue*) and after 5 minutes of bath application of 1 µM glucagon (*bottom, orange*), in the treated eye of a 3-week negative lens exposed mouse. (**G**) No change was observed in the average frequency of glycinergic IPSCs (Wilcoxon signed-rank test), with a decrease in average amplitude (Wilcoxon signed-rank test) (**H**) and no change in decay times (paired *t* test) (**I**). (**J**) Representative traces of RBC IPSCs under control conditions (*left, blue*), after 15 minutes of bath application of 10 µM SKF 81297 (*middle, orange*) and after 5 minutes of bath application of 10 µM SKF 81297 + 1 µM glucagon (*right, green*), in the treated eye of a 3-week negative lens exposed mouse. (**K**) Application of SKF 81297 alone increased average IPSC frequency, with a further increase when glucagon was added (Friedman test with Durbin-Conover pairwise comparisons). Co-application of SKF 81297 and glucagon produced a decrease in IPSC amplitude (Friedman test with Durbin-Conover pairwise comparisons) (**L**). No change was observed in the average decay times (repeated measures ANOVA) (**M**).

Investigative Ophthalmology & Visual Science

were co-applied (control = 12.04 ± 9.05 pA, SKF = 6.76 ± 1.64 pA, and SKF + glucagon = 5.55 ± 1.64 pA, $P = 0.005$, $n = 7$; Fig. 3L). No change was observed in the average decay time (Fig. 3M). These results suggest that dopaminergic agonism through D1R alone can increase the frequency of inhibitory activity after 3 weeks of negative lens exposure, and furthermore rescue the effect of glucagon on this activity.

Discussion

The main effect of the application of glucagon in the present study was an increase in RBC inhibitory activity, reflecting stronger inhibitory signaling onto these cells. To the best of our knowledge, no previous reports exist for this effect, as the role of glucagon in the central nervous system (CNS) has been mostly studied regarding its metabolic effects.[42] However, the highly related GLP-1[43] has been shown, for example, to modulate glutamate release in mouse lateral hypothalamus[44] and to increase the release of glutamate in rat basal ganglia,[45] representing a precedent for a role of members of the secretin/glucagon family as neuromodulators in the CNS.

RBCs could be separated based on the effect on IPSC frequency of glucagon into 2 groups, with the cells showing more than 10% change over baseline having larger somas and axons. This partially correlates with the classification by Tsukamoto and Omi,[46] as RBC subtypes RB1 and RB2 were grouped based on their axon length within the IPL. However, more detailed functional and histochemical markers will be necessary to more precisely define the RBC subtypes involved.

The application of the glucagon receptor antagonist L-168,049 produced the abolition of the effect of glucagon, suggesting that glucagon is acting through its canonical receptor. However, application of L-168,049 was also associated with a decrease in the amplitude of IPSCs and a shift to higher decay times. This could be related to off-target effects, due to the high similarity of the receptors in the secretin/glucagon family,[47] as L168,049 is an allosteric antagonist. Combined with the fact that the concentration of glucagon used was high compared to other studies,[5] this opens the possibility of another member of the secretin/glucagon family to be the one whose receptors are mediating the observed effects, which should be the subject of further investigation. Out of the many members of this family, VIP seems to be the most likely candidate, as this molecule has been linked to myopia in both mice[48] and humans.[48,49]

Dopamine has been shown to control the inhibitory activity of RBCs,[33,39] thus the present study tested the possible interplay between dopaminergic neuromodulation of RBC inhibitory activity and its regulation by glucagon, as this interaction could provide hints about the pathophysiology of myopia. On one hand, D1R antagonism produced the abolition of the effect of glucagon on IPSC frequency, suggesting a dependence of glucagon on this signaling pathway. On the other hand, D2R antagonism increased the frequency of IPSCs by itself, but co-application of glucagon produced a further increase, suggesting that both pathways are independent. Furthermore, under scotopic conditions, an overall hypodopaminergic state based on our HPLC measurements and previous reports,[40] the effects on IPSC frequency were comparable to those seen under D1R antagonism. Overall, this suggests an interaction between glucagonergic and dopaminergic signaling in the mammalian retina, the effect of glucagon application being dependent on dopaminergic activity. Although no previous data exist for this particular effect, interactions between dopamine and molecules from the secretin/glucagon family have been shown in other areas of the CNS.[50,51]

In the case of the mice treated with a negative lens, after 3 weeks of lens exposure, the effect of glucagon was abolished, a situation similar to that seen under D1R antagonism and under scotopic conditions, which can be related to an alteration of dopaminergic activity, as has been previously reported under similar myopia-inducing conditions.[15] An unexpected observation was a decrease in the average amplitude of IPSCs in the control eye, even though it was not statistically significant, this could be due to a restricted sample size, and could be related to recent reports of contralateral changes in the unexposed eyes of negative-lens exposed mice.[52]

In addition, D1R agonism was able to recover the effect of glucagon under this negative-lens exposure, with an increase in frequency with D1R agonism, and a further increase with the addition of glucagon. It is important to note, however, that because refractive error measurements were not performed in the current study, it was not possible to ascertain whether the animals effectively developed myopia.

Nevertheless, the results obtained show a link among negative lens exposure, dopaminergic disfunction, and the abolition of the effect of glucagon, and further support the necessity of D1R activity for glucagon to exert its effects. To clarify whether this is due to a dopaminergic alteration associated with myopia-inducing treatment will require further study. This link with D1R activity is also of interest, as even though the differential role of both dopamine receptor families in myopia is not clear, there is evidence supporting D1R signaling as a key mediator of different protective interventions in myopia, such as light,[53] apomorphine,[26] and unrestricted vision,[20] making it an interesting target for future treatments.

The specific circuitry underlying the glucagonergic-dopaminergic interaction is a hard question to answer. Previous studies have failed to find glucagonergic amacrine cells in the mouse retina as opposed to the avian retina,[54] and reports regarding the presence of glucagon and its receptor in the murine retina are scarce and conflicting,[55] making it difficult to pinpoint the possible origin of a putative retinal glucagon release. Furthermore, as discussed before, the amacrine cells in charge of the observed effect could in turn correspond to VIPergic amacrine cells.[54] As dopaminergic antagonism and hypodopaminergic conditions abolish the effect of glucagon, dopaminergic signaling through D1R seems to be downstream of glucagon. However, the specific cell types involved cannot be determined with the data from this study.

It is interesting to note how SKF 81297 increases IPSC frequency by itself in the lens-exposed animals, but the subsequent application of glucagon increases the frequency even more, suggesting 2 different sources of activity. Whether this interaction involves inhibitory amacrine cells acting as interneurons between both signaling systems as previously described for GABAergic signaling and D1R expressing interneurons,[33,39] a direct modulation of dopaminergic amacrine cells by glucagon, consistent, for example, with previous reports of neurons co-expressing tyrosine hydroxylase and VIP,[56] or the modulation of intracellular pathways in the target cell, as both receptors share

intracellular pathways,[57,58] remains an interesting question that also requires further study.

Overall, the physiological data and pharmacological analysis of the present study support the presence of glucagon-like activity in the mouse retina, specifically increasing the frequency of the inhibitory activity acting on RBCs under photopic conditions. This is the first description of such an effect in the CNS, as no electrophysiological or other functional studies have previously reported an effect of glucagon on the mammalian retina. This glucagonergic activity is in turn dependent on dopaminergic signaling through D1R, as its specific antagonism and conditions associated with low dopamine levels, such as scotopic conditions, prevent the effect of glucagon. Moreover, this interaction is disrupted in negative lens exposed mice, with an abolition of the effect of glucagon that can be rescued using D1R agonism. These results reveal an interaction pathway between glucagon and dopamine in the inner retina, with possible relevance for retinal signal processing.

Acknowledgments

Supported by the Chilean government through ANID PhD fellowship #21171887 to F.T., ANID-FONDECYT #11191211 to A.H.V., #1210790 to O.S. and #1200474 to R.S-Z., DIUV-CI Grant #01/2006 to R.S.-Z. and the Center for Mathematical Modelling (CMM) #FB210005 to F.T.

Disclosure: **F. Tapia**, None; **V. Peñaloza**, None; **F. Silva-Olivares**, None; **R. Sotomayor-Zárate**, None; **O. Schmachtenberg**, None; **A.H. Vielma**, None

References

1. Denes V, Hideg O, Nyisztor Z, et al. The neuroprotective peptide PACAP1-38 contributes to horizontal cell development in postnatal rat retina. *Invest Opthalmol Vis Sci*. 2019;60(2):770.
2. Feldkaemper MP, Schaeffel F. Evidence for a potential role of glucagon during eye growth regulation in chicks. *Vis Neurosci*. 2002;19(6):755–766.
3. Fischer AJ, Skorupa D, Schonberg DL, Walton NA. Characterization of glucagon-expressing neurons in the chicken retina. *J Comp Neurol*. 2006;496(4):479–494.
4. Sterling JK, Adetunji MO, Guttha S, et al. GLP-1 receptor agonist NLY01 reduces retinal inflammation and neuron death secondary to ocular hypertension. *Cell Rep*. 2020;33(5):108271.
5. Vessey KA, Rushforth DA, Stell WK. Glucagon- and secretin-related peptides differentially alter ocular growth and the development of form-deprivation myopia in chicks. *Invest Ophthalmol Vis Sci*. 2005;46(11):3932–3942.
6. Holden BA, Fricke TR, Wilson DA, et al. Global prevalence of myopia and high myopia and temporal trends from 2000 through 2050. *Ophthalmology*. 2016;123(5):1036–1042.
7. Ma M, Xiong S, Zhao S, Zheng Z, Sun T, Li C. COVID-19 home quarantine accelerated the progression of myopia in children aged 7 to 12 years in China. *Invest Opthalmol Vis Sci*. 2021;62(10):37.
8. Zhu X, Wallman J. Opposite effects of glucagon and insulin on compensation for spectacle lenses in chicks. *Invest Opthalmol Vis Sci*. 2009;50(1):24.
9. Vessey KA, Lencses KA, Rushforth DA, Hruby VJ, Stell WK. Glucagon receptor agonists and antagonists affect the growth of the chick eye: a role for glucagonergic regulation of emmetropization? *Invest Opthalmol Vis Sci*. 2005;46(11):3922.
10. Bitzer M, Schaeffel F. Defocus-induced changes in ZENK expression in the chicken retina. *Invest Ophthalmol Vis Sci*. 2002;43(1):246–252.
11. Ashby R, Kozulin P, Megaw PL, Morgan IG. Alterations in ZENK and glucagon RNA transcript expression during increased ocular growth in chickens. *Mol Vis*. 2010;16:639–649.
12. Schippert R, Burkhardt E, Feldkaemper M, Schaeffel F. Relative axial myopia in Egr-1 (ZENK) knockout mice. *Invest Ophthalmol Vis Sci*. 2007;48(1):11–17.
13. Zhong X, Ge J, Smith EL, Stell WK. Image defocus modulates activity of bipolar and amacrine cells in macaque retina. *Invest Ophthalmol Vis Sci*. 2004;45(7):2065–2074.
14. Ashby RS, Zeng G, Leotta AJ, Tse DY, McFadden SA. Egr-1 mRNA expression is a marker for the direction of mammalian ocular growth. *Invest Opthalmol Vis Sci*. 2014;55(9):5911.
15. Zhou X, Pardue MT, Iuvone PM, Qu J. Dopamine signaling and myopia development: what are the key challenges. *Prog Retin Eye Res*. 2017;61:60–71.
16. Landis EG, Park HN, Chrenek M, et al. Ambient light regulates retinal dopamine signaling and myopia susceptibility. *Invest Opthalmol Vis Sci*. 2021;62(1):28.
17. Dong F, Zhi Z, Pan M, et al. Inhibition of experimental myopia by a dopamine agonist: different effectiveness between form deprivation and hyperopic defocus in guinea pigs. *Mol Vis*. 2011;17:2824–2834.
18. McCarthy CS, Megaw P, Devadas M, Morgan IG. Dopaminergic agents affect the ability of brief periods of normal vision to prevent form-deprivation myopia. *Exp Eye Res*. 2007;84(1):100–107.
19. Nickla DL, Totonelly K, Dhillon B. Dopaminergic agonists that result in ocular growth inhibition also elicit transient increases in choroidal thickness in chicks. *Exp Eye Res*. 2010;91(5):715–720.
20. Nickla DL, Totonelly K. Dopamine antagonists and brief vision distinguish lens-induced- and form-deprivation-induced myopia. *Exp Eye Res*. 2011;93(5):782–785.
21. Huang F, Yan T, Shi F, et al. Activation of dopamine D2 receptor is critical for the development of form-deprivation myopia in the C57BL/6 mouse. *Invest Opthalmol Vis Sci*. 2014;55(9):5537.
22. Wu XH, Li YY, Zhang PP, et al. Unaltered retinal dopamine levels in a C57BL/6 mouse model of form-deprivation myopia. *Invest Ophthalmol Vis Sci*. 2015;56(2):967–977.
23. Qian KW, Li YY, Wu XH, et al. Altered retinal dopamine levels in a melatonin-proficient mouse model of form-deprivation myopia. *Neurosci Bull*. 2022;38(9):992–1006.
24. Landis EG, Chrenek MA, Chakraborty R, et al. Increased endogenous dopamine prevents myopia in mice. *Exp Eye Res*. 2020;193:107956.
25. Wu XH, Qian KW, Xu GZ, et al. The role of retinal dopamine in C57BL/6 mouse refractive development as revealed by intravitreal administration of 6-hydroxydopamine. *Invest Opthalmol Vis Sci*. 2016;57(13):5393.
26. Huang F, Zhang L, Wang Q, et al. Dopamine D1 receptors contribute critically to the apomorphine-induced inhibition of form-deprivation myopia in mice. *Invest Ophthalmol Vis Sci*. 2018;59(6):2623–2634.
27. Shu Z, Chen K, Wang Q, et al. The role of retinal dopamine D1 receptors in ocular growth and myopia development in mice. *J Neurosci*. Published online September 26, 2023:JN-RM-1196-23, doi:10.1523/JNEUROSCI.1196-23.2023.
28. Huang F, Shu Z, Huang Q, et al. Retinal dopamine D2 receptors participate in the development of myopia in mice. *Invest Opthalmol Vis Sci*. 2022;63(1):24.
29. Huang F, Wang Q, Yan T, et al. The Role of the dopamine D2 receptor in form-deprivation myopia in mice: studies with

full and partial D2 receptor agonists and knockouts. *Invest Opthalmol Vis Sci*. 2020;61(6):47.
30. Ashby R, McCarthy CS, Maleszka R, Megaw P, Morgan IG. A muscarinic cholinergic antagonist and a dopamine agonist rapidly increase ZENK mRNA expression in the form-deprived chicken retina. *Exp Eye Res*. 2007;85(1):15–22.
31. Park H na, Jabbar SB, Tan CC, et al. Visually-driven ocular growth in mice requires functional rod photoreceptors. *Invest Opthalmol Vis Sci*. 2014;55(10):6272.
32. Eggers ED, Mazade RE, Klein JS. Inhibition to retinal rod bipolar cells is regulated by light levels. *J Neurophysiol*. 2013;110(1):153–161.
33. Flood MD, Moore-Dotson JM, Eggers ED. Dopamine D1 receptor activation contributes to light-adapted changes in retinal inhibition to rod bipolar cells. *J Neurophysiol*. 2018;120(2):867–879.
34. Fischer AJ, McGuire JJ, Schaeffel F, Stell WK. Light-and focus-dependent expression of the transcription factor ZENK in the chick retina. *Nat Neurosci*. 1999;2(8):705–712.
35. Ghosh KK, Bujan S, Haverkamp S, Feigenspan A, Wässle H. Types of bipolar cells in the mouse retina. *J Comp Neurol*. 2004;469(1):70–82.
36. Vielma AH, Schmachtenberg O. Electrophysiological fingerprints of OFF bipolar cells in rat retina. *Sci Rep*. 2016;6(1):30259.
37. Elgueta C, Leroy F, Vielma AH, Schmachtenberg O, Palacios AG. Electrical coupling between A17 cells enhances reciprocal inhibitory feedback to rod bipolar cells. *Sci Rep*. 2018;8(1):3123.
38. Ivanova E, Müller U, Wässle H. Characterization of the glycinergic input to bipolar cells of the mouse retina. *Eur J Neurosci*. 2006;23(2):350–364.
39. Travis AM, Heflin SJ, Hirano AA, Brecha NC, Arshavsky VY. Dopamine-dependent sensitization of rod bipolar cells by GABA is conveyed through wide-field amacrine cells. *J Neurosci*. 2018;38(3):723–732.
40. Pérez-Fernández V, Milosavljevic N, Allen AE, et al. Rod photoreceptor activation alone defines the release of dopamine in the retina. *Curr Biol*. 2019;29(5):763–774.e5.
41. Jiang X, Kurihara T, Kunimi H, et al. A highly efficient murine model of experimental myopia. *Sci Rep*. 2018;8(1):1–12.
42. Abraham MA, Lam TKT. Glucagon action in the brain. *Diabetologia*. 2016;59(7):1367–1371.
43. Adelhorst K, Hedegaard BB, Knudsen LB, Kirk O. Structure-activity studies of glucagon-like peptide-1. *J Biol Chem*. 1994;269(9):6275–6278.
44. Acuna-Goycolea C. Glucagon-like peptide 1 excites hypocretin/orexin neurons by direct and indirect mechanisms: implications for viscera-mediated arousal. *J Neurosci*. 2004;24(37):8141–8152.
45. Mora F, Expösito I, Sanz B, E. B. Selective release of glutamine and glutamic acid produced by perfusion of GLP-1(7–36) amide in the basal ganglia of the conscious rat. *Brain Res Bull*. 1992;29(3–4):359–361.
46. Tsukamoto Y, Omi N. Classification of mouse retinal bipolar cells: type-specific connectivity with special reference to rod-driven AII amacrine pathways. *Front Neuroanat*. 2017;11:1–25.
47. Tam JKV, Lee LTO, Jin J, Chow BKC. Molecular evolution of GPCRs: secretin/secretin receptors. *J Mol Endocrinol*. 2014;52(3):T1–T14.
48. Zhao F, Li Q, Chen W, et al. Dysfunction of VIPR2 leads to myopia in humans and mice. *J Med Genet*. 2022;59(1):88–100.
49. Tedja MS, Wojciechowski R, Hysi PG, et al. Genome-wide association meta-analysis highlights light-induced signaling as a driver for refractive error. *Nat Genet*. 2018;50(6):834–848.
50. Eren-Yazicioglu CY, Yigit A, Dogruoz RE, Yapici-Eser H. Can GLP-1 be a target for reward system related disorders? A qualitative synthesis and systematic review analysis of studies on palatable food, drugs of abuse, and alcohol. *Front Behav Neurosci*. 2021;14:614884.
51. Szadai Z, Pi HJ, Chevy Q, et al. Cortex-wide response mode of VIP-expressing inhibitory neurons by reward and punishment. *Elife*. 2022;11:e78815.
52. Ma Z, Jeong H, Yang Y, et al. Contralateral effect in progression and recovery of lens-induced myopia in mice. *Ophthalmic Physiol Opt*. 2023;43(3):558–565.
53. Chen S, Zhi Z, Ruan Q, et al. Bright light suppresses form-deprivation myopia development with activation of dopamine D1 receptor signaling in the ON pathway in retina. *Invest Opthalmol Vis Sci*. 2017;58(4):2306.
54. Mathis U, Schaeffel F. Glucagon-related peptides in the mouse retina and the effects of deprivation of form vision. *Graefes Arch Clin Exp Ophthalmol*. 2007;245(2):267–275.
55. Feldkaemper M, Burkhardt E, Schaeffel F. Localization and regulation of glucagon receptors in the chick eye and preproglucagon and glucagon receptor expression in the mouse eye. *Exp Eye Res*. 2004;79(3):321–329.
56. Asmus SE, Cocanougher BT, Allen DL, et al. Increasing proportions of tyrosine hydroxylase-immunoreactive interneurons colocalize with choline acetyltransferase or vasoactive intestinal peptide in the developing rat cerebral cortex. *Brain Res*. 2011;1383:108–119.
57. Janah L, Kjeldsen S, Galsgaard KD, et al. Glucagon receptor signaling and glucagon resistance. *Int J Mol Sci*. 2019;20(13).
58. Neve KA, Seamans JK, Trantham-Davidson H. Dopamine receptor signaling. *J Recept Signal Transduct Res*. 2004;24(3):165–205.

Investigative Ophthalmology & Visual Science